

Binding of HgCl₂ by a Nitro Functionalized Tripodal Receptor and Its Decomplexation Controlled by Anion Complexation

Sandeep Kumar Dey^[a] and Gopal Das^{*[a]}

Keywords: Mercury / Hydrogen bonds / Anions / Anionic templates / Tripodal receptor / Molecular transformation

The presence of a nitro functionality on *N*-bridged tripodal receptors has an effect on its binding ability towards HgCl₂ by coordination through one of the nitro oxygen atoms, etheral oxygen and the bridgehead nitrogen atom. Decomplexation of HgCl₂ and recovery of the receptor **L** can be accomplished by the formation of anion complexes with [L·HgCl₂]. The complexation of different anions with multiple protonated receptor units is attributable to intramolecular (N–H)⁺···anion interactions, at the same time the presence

of multiple C–H···anion and interligand C–H···O_{nitro} hydrogen bonds provide added stabilization. Protonation at the bridgehead nitrogen atom and the presence of the nitro functionality render the aliphatic and aryl protons sufficiently acidic for their active participation in moderate to weak C–H···anion and C–H···O_{nitro} interactions. Spectroscopic studies provide evidence for the formation of anion complexes from [L·HgCl₂] by extrusion of HgCl₂.

Introduction

Podands, cavitands, hemicarcerands and capsules are interesting members of the receptor family, in which the confined interior space (or cavity) formed either by self-assembly of the monomeric unit through noncovalent interactions or by metal–ligand coordination, have been employed in various applications.^[1] The use of anionic templates for the synthesis of superstructures has become an attractive strategy in recent years.^[2] However, the strategic use of anion binding as a driving force for templated assembly by decomplexation of metal complexes is rare. Hydrogen bonds formed with anions are weaker and more difficult to control than metal–cation coordination bonds. Thus, anion template-induced transformation of molecular species represents a new approach in the control of supramolecular assembly formation.^[3] Although numerous synthetic molecular transformations have been achieved by the variation of an integral part of supramolecular aggregates, it is still a challenge to control the assembly and transformation processes when a guest acts as a template.

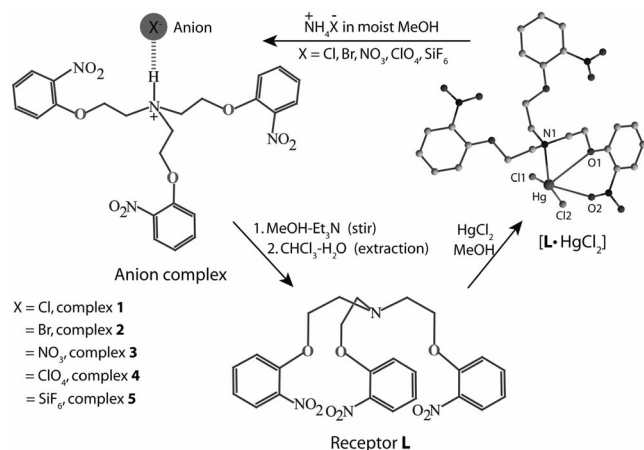
In the present study, we report an *ortho*-nitro functionalized tripodal receptor possessing O- and N-donors (Scheme 1) that reversibly bind Hg²⁺ and form the basis for anion templated supramolecular self-assembly of a tripodal ligand by decomplexation of the Hg complex. In all reported Hg^{II} complexes of tripodal ether ligands, the ligand

is bound to HgCl₂ through the bridgehead N and one or two etheral O atoms from the flexible side arms, depending upon the position (*ortho*, *meta* or *para*) of the substituents in the terminal phenyl ring.^[4] However, we report here the unusual participation of a nitro oxygen atom from one of the flexible arms of the podand binding the Hg²⁺ as well as the conventional N (apical) and O (etheral) donor atoms. The binding ability of Hg²⁺ towards etheral oxygen and nitrogen donors is well known and its structural versatility is displayed by Hg^{II}_xCl_yⁿ⁻ anions.^[5] Tripodal ligands are likely to form complexes that are thermodynamically stable and kinetically not labile. However, the tertiary nitrogen of *N*-bridged tripodal podands is susceptible to protonation and the hydrogen of the protonated nitrogen atom could become *exo*- or *endo*-orientated with respect to the side arms depending on the nature of the anion.^[6] Thus, the counter anion(s) could play an important role in assembling and controlling the structural topologies of the podands in the solid state.^[7] Moreover, by varying the geometry of the anions involved in the self-assembly of a receptor, it should be possible to reorient or rupture the self-assembled architectures based on the number of hydrogen bonding contacts required by different anions. Recently, we have demonstrated the aryl azo imidazole-assisted assembly of anion–water through salt formation in the presence of mildly acidic ammonium salts and have also explored the charge assisted complexation of anions of varied dimensionality by a *para*-nitro-functionalized tripodal podand.^[8] Thus, we have made an attempt to explore the transformation of a tripodal metal complex with mercury into supramolecular complexes with anions by extrusion of HgCl₂, employing mildly acidic ammonium salts as decomplexation agents in moist MeOH (Scheme 1). Furthermore, the tripodal recep-

[a] Department of Chemistry, Indian Institute of Technology Guwahati, North Guwahati, Assam 781039, India
Fax: +91-361-258-2349
E-mail: gdas@iitg.ernet.in

Supporting information for this article is available on the WWW under <http://dx.doi.org/10.1002/ejic.201000825>.

tor can be recovered in good yield by stirring a methanolic solution of the anion complex in the presence of excess Et_3N .



Scheme 1. Schematic representation of the reversible binding of HgCl_2 by **L** controlled by anion complexation.

Results and Discussion

Single-Crystal X-ray Structural Study of $[\text{L}\cdot\text{HgCl}_2]$

The tripodal ligand **L** readily reacts with HgCl_2 at room temperature, in MeOH affording a five-coordinate Hg^{II} complex which crystallizes in the monoclinic space group $P2_1/c$ with $Z = 4$. An ORTEP plot of $[\text{L}\cdot\text{HgCl}_2]$ complex is depicted in part a of Figure 1 with the atom numbering scheme. The ligand is bound to HgCl_2 through the bridge-head N atom and one of the ethereal oxygen atoms O1 in the flexible side arm of the podand ($\text{N1}\cdots\text{Hg1}$ 2.554 Å; $\text{O1}\cdots\text{Hg1}$ 3.029 Å). In addition, the nitro oxygen atom O2 from the same arm is coordinated to HgCl_2 with a bond length of 2.728 Å. The unusual coordination mode of the nitro oxygen atom with HgCl_2 is possibly due to the inward orientation of the coordinating nitro group towards HgCl_2 resulting in the formation of a six-membered ring that includes the coordinated ethereal oxygen O1. One oxygen atom from each of the noncoordinating nitro groups O6 and O8 is involved in interligand C–H \cdots O interactions with the alkyl hydrogen atoms H10B and H5, respectively ($\text{C10}\cdots\text{O6}$ 3.336 Å; $\text{C5}\cdots\text{O8}$ 3.402 Å). The aromatic hydrogen atom H6 from the coordinating side arm is involved in a weak dimeric interaction with the chlorine atom Cl1 of the adjacent $[\text{L}\cdot\text{HgCl}_2]$ unit through C–H \cdots Cl hydrogen bonds (3.865 Å) and face to face ($\pi\cdots\pi$) interactions between the identical phenyl rings ($\text{C1g}\cdots\text{C1g}$ 4.121 Å). Furthermore, each dimeric unit interacts with two other dimers through aliphatic C–H \cdots π interactions and $\pi\cdots\pi$ stacking (Figure 1, b). The aliphatic H2B protons of the coordinating side arm and H18B from a noncoordinating side arm of a dimeric unit interact with the phenyl rings (through C1g and C2g) of two different units with bond distances of 4.041 and 3.708 Å.

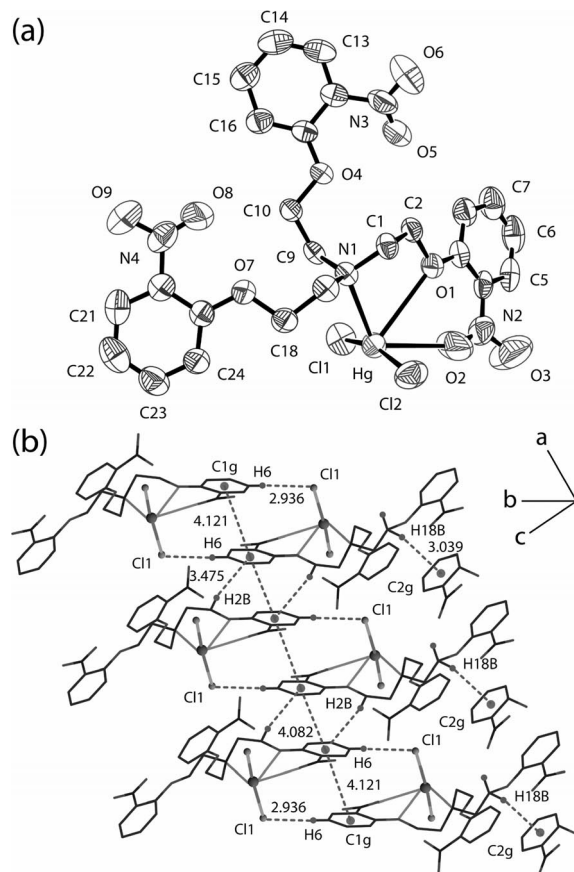


Figure 1. (a) ORTEP plot (50% probability ellipsoids) of $[\text{L}\cdot\text{HgCl}_2]$; (b) ball and stick representation of the C–H \cdots Cl hydrogen bonded dimeric units with relevant hydrogen bond lengths. Selected bond [Å] and angle ($^\circ$) parameters for $[\text{L}\cdot\text{HgCl}_2]$: $\text{N1}\cdots\text{Hg1}$ 2.554(4), $\text{O1}\cdots\text{Hg1}$ 3.029, $\text{O2}\cdots\text{Hg1}$ 2.728, $\text{Hg1}\cdots\text{Cl1}$ 2.3083(16), $\text{Hg1}\cdots\text{Cl2}$ 2.3154(16), $\text{Cl1}\cdots\text{Hg1}\cdots\text{Cl2}$ 162.82(7), $\text{Cl1}\cdots\text{Hg1}\cdots\text{N1}$ 101.94(9), $\text{Cl2}\cdots\text{Hg1}\cdots\text{N1}$ 94.36(9).

Formation of Anion Complexes by Decomplexation of HgCl_2

When a methanolic solution of the Hg complex is treated with 1 equiv. an ammonium salt [NH_4Cl , NH_4Br , NH_4NO_3 , NH_4ClO_4 or $(\text{NH}_4)_2\text{SiF}_6$] it forms a supramolecular complex of the anion by extrusion of Hg^{2+} from the complex as HgCl_2 . The ammonium ion is mildly acidic and reacts with Brønsted bases (i.e., the *N*-bridged podand) and return to ammonia. After stirring for 4 h with heating, the yellow solution became colourless, was filtered and left undisturbed in a beaker to crystallize. Slow evaporation of the solvent at room temperature afforded colourless crystals of the anion complexes in greater than 75% yields.

Structural information obtained from single-crystal X-ray analysis of the anionic complexes provides an insight into the binding topology of anions with the protonated tripodal podand receptor and the nature of the intermolecular hydrogen bond-directed self-assembly of the complexes. In the supramolecular complexes, independent of the geometry and charge of the anion, the **L**:anion stoichiometry is 1:1 except for $[\text{HL}^+][0.5\text{SiF}_6^{2-}]$ (**5**), which has a

2:1 L:anion ratio. Complexation with different anions by **L** is principally governed by two different types of supra-molecular interactions. In all complexes, the *exo*-orientated hydrogen atom of the protonated bridgehead nitrogen atom of **L** participate in a comparatively strong intramolecular (N–H)⁺⋯anion bonding as hydrogen-bond donors. In addition to the (N–H)⁺⋯anion interaction, the anions are further involved in several C–H⋯anion interactions with different alkyl and aryl hydrogen atoms from the protonated podand satisfying the geometrical necessity of the flexible LH⁺ units to respond to the demands of anions of different sizes and geometries. The complexes are further stabilized by various weak interligand directional hydrogen bonds, which induce rigidity in the cationic podand formed and serve as the foundation for the selective crystallization of desired salts.

Single-Crystal X-ray Structural Studies of Anion Complexes

The chloride complex [HL⁺][Cl⁻] (**1**) crystallizes in the monoclinic space group *P*2₁/*c*, with *Z* = 4. The hydrogen atom of the protonated apical nitrogen is *exo*-orientated with respect to the tripodal arms. The torsion angles (τ_{ether}) involving N1_{amino}–C–C–O_{ether} are all in the folded conformation for the three tripodal arms (Table S4). A magnified view of the hydrogen bonding interactions with the chloride ion together with the relevant edge-to-face interactions, shown in Figure 2 (a), demonstrates that each chloride anion is involved in a three-point attachment provided by three LH⁺ units with two C–H⋯Cl⁻ contacts. The *exo*-orientated proton H1N is involved in an intramolecular (N–H)⁺⋯Cl⁻ interaction with the anion with a hydrogen bonding distance of 3.015 Å and a N–H⋯Cl angle of 165°. The aliphatic hydrogen atom H9A and aryl hydrogen atom H14 of two different units make weak intermolecular C–H⋯Cl⁻ contacts with hydrogen bonding distances of 3.645 and 3.598 Å, respectively (Table S2). The C–H⋯Cl angle of 140° further implies the comparatively weak nature of the C–H hydrogen bonds involving hydrogen atoms H9A and H14 (Table S2). The crystal packing diagram viewed along the *b*-axis (Figure 2, b) reveals that the receptor molecules pack in a bilayer array forming a hydrophobic chain of ligand moieties. The chloride ions are trapped between the adjacent bilayers generating a hydrophilic chain parallel to the *c*-axis. Intermolecular C–H⋯O_{nitro} hydrogen bonding between alkyl hydrogen atom H18B and nitro oxygen atom O2 (C18⋯O2 3.630 Å, C18–H18B⋯O2 163°) bridges the receptor moieties along the *c*-axis. The adjacent monolayers of the ligand array are further connected through C–H⋯O_{nitro} hydrogen bonds involving the aryl hydrogen atom H23 with the nitro oxygen atom O6 (C23⋯O6 3.401 Å, C23–H23⋯O6 155°) and interligand edge to face (C–H⋯ π) interactions between the aliphatic hydrogen atom H1B with the phenyl ring involving carbon atoms C3–C8 (C1⋯C1g 4.258 Å, C1–H1B⋯C1g 120°) forming bilayers along *c*-axis. Two such bilayers are themselves interlinked by C–H⋯ π in-

teractions between the aliphatic hydrogen atom H17B and the phenyl ring carbon atoms C19–C24 (C17⋯C3g 3.970 Å, C17–H17B⋯C3g 134°).

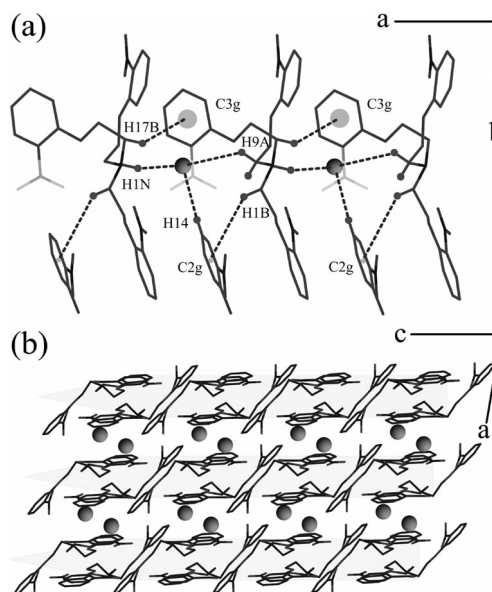


Figure 2. (a) Magnified view of the three hydrogen-bonding contacts on the chloride anion (dashed lines) with three LH⁺ units with the interligand C–H⋯ π interactions; (b) crystal packing diagram of **1** viewed down the *b*-axis showing the bilayer assembly formation of cationic ligand moieties along the *c*-axis with the chloride anions situated between the adjacent bilayers.

The bromide complex [HL⁺][Br⁻] (**2**) crystallizes in the lower symmetry triclinic space group *P* $\bar{1}$ with *Z* = 2. The torsion τ_{ether} involving N1_{amino}–C–C–O_{ether} is in the folded conformation for two side arms composed of the ethereal oxygen atoms O1 and O4 and is in the extended conformation for the third arm composed of the ethereal oxygen atom O7 (Table S4). Similar to **1**, the bromide ion is involved in a three-point hydrogen bond contact provided by three encircling cationic tripodal units. In addition to the electrostatic (N–H)⁺⋯Br⁻ interaction (N⋯Br 3.303 Å, N–H⋯Br 150°), the aliphatic hydrogen atom H1A and aryl hydrogen atom H7 of two different tripodal units are engaged in forming weak intermolecular C–H⋯Br⁻ contacts with hydrogen bonding distances of 3.566 and 3.730 Å, respectively. The C–H⋯Br angles of 129 and 133° suggest the feeble nature of the C–H hydrogen bonds (Table S2). A magnified view of the bromide binding with relevant contact distances is depicted in Figure 3. The unusual three-point contacts in both **1** and **2** suggest that the interactions with the C–H donors are too weak to impose a definite coordination structure around the halide anions, and instead the C–H groups on the flexible arms of the receptor embrace the anion so as to match its size and shape to provide a favourable electrostatic environment around it. The cationic tripodal units are self assembled by four intermolecular C–H⋯O_{nitro} interactions between different alkyl and aryl hydrogen atoms (H2B, H10A, H12 and H21) and one of the oxygen atoms (O3, O6 and O9) from each nitro group with an average hydrogen bond length of 3.255 Å,

where O9 acts as a bifurcated hydrogen-bond acceptor (Table S3). In addition, the tripodal cations are cross-linked by means of an interligand edge to face interaction between aryl hydrogen atom H5 and the phenyl ring carbon atoms C18–C24 (C5...C3g 3.886 Å, C5–H5...C3g 130°) and a face to face interaction between two identical phenyl rings (C3g...C3g 3.694 Å) of adjacent tripodal cations forming a bilayer assembly of ligand moieties (Supporting Information).

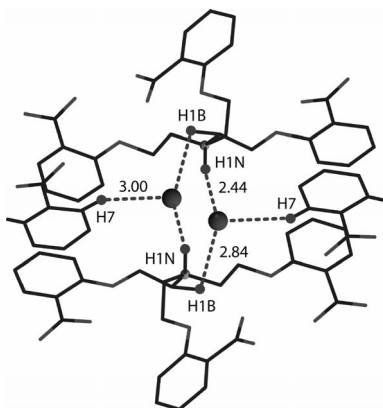


Figure 3. Magnified view of the three hydrogen bonding interactions involving the bromide anion (dashed lines) with three neighbouring LH^+ units.

The nitrate complex $[\text{LH}^+][\text{NO}_3^-] \cdot 0.5\text{H}_2\text{O}$ (**3**) crystallizes in the orthorhombic space group $Pbcn$ with $Z = 4$. The structure of the salt comprises a protonated tripodal cation with NO_3^- and half a water molecule as solvent of crystallization. The solid-state structure of **3** shows a bifurcated ($\text{N}-\text{H}$) $^+ \cdots \text{O}$ interaction between the hydrogen atom H1N of the protonated amine with the nitrate oxygen atoms O10 and O12 through $\text{N} \cdots \text{O}$ distances measuring 2.809 and 3.299 Å and $\text{N}-\text{H} \cdots \text{O}$ angles of 166 and 136°, respectively. In addition, the nitrate oxygen atoms are C–H hydrogen bonded to four encircling podand molecules with an average hydrogen bonding distance of 3.390 Å (ranging from 3.259 to 3.626 Å) and C–H...O angles between 131 and 175° (Table S2). The nitrate oxygen atom O10 is involved in a moderate aliphatic C–H...O interaction with the methylene hydrogen atom H10A (C10...O10 3.259 Å, C10–H10A...O10 139°) of the same tripodal unit forming bifurcated ($\text{N}-\text{H}$) $^+ \cdots \text{O}$ hydrogen bonds. The lattice water molecule (O13w) displays bridge hydrogen bonding with the oxygen atom O10 of two adjacent nitrate anions through hydrogen bonds measuring 2.953 Å, forming a nitrate–water–nitrate adduct (Figure 4, a). Two arms of each cationic L unit are projected in one direction to form a cleft shaped cavity and two such tripodal clefts intercalate face to face to encapsulate the water bridged nitrate–water–nitrate adduct. The water molecule is further engaged in bifurcated C–H...O hydrogen bond formation with the aliphatic proton H10A of the individual tripodal cations stabilizing the trapped nitrate and water molecules within the tripodal cleft. O11 is C–H hydrogen bonded to two aryl protons (H6 and H20), whereas the methylene proton H9A and aryl proton H7 make contacts

with O12 through weak C–H...O hydrogen bonds completing the eight-point contacts that stabilize the nitrate in the receptor channel (Figure 4, b). The cationic ligand moieties are self-organized by four interligand C–H...O_{nitro} hydrogen bonds between different aliphatic protons (H1B, H9A, H9B and H10B) and one of the oxygen atoms (O3, O6 or O9) from each nitro group, where O9 behaves as bifurcated hydrogen-bond acceptor. Intermolecular C–H...O_{nitro} hydrogen bonding between the alkyl hydrogen H1B and nitro oxygen O3 (C1...O3 3.224 Å, C1–H1B...O3 125°) bridges the tripodal molecules in a zigzag fashion forming bilayers along the a -axis. Adjacent bilayers of the ligand array are further interconnected through C–H...O_{nitro} hydrogen bonding interactions involving the aliphatic hydrogen atoms H9A and H10B with the nitro oxygen atoms O9 and O6 (Supporting Information).

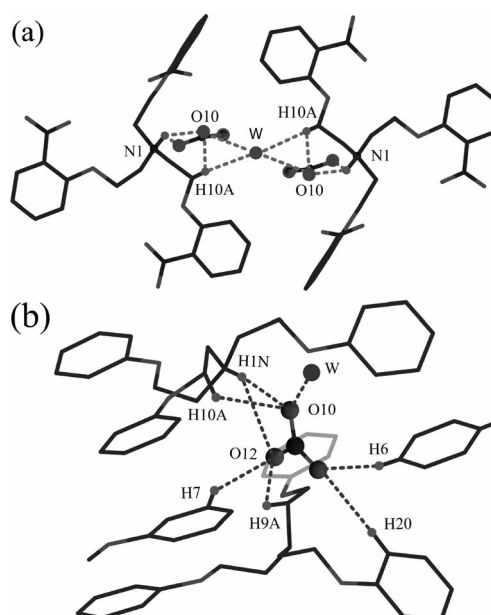


Figure 4. (a) Crystal structure of **3** depicting the encapsulation of the nitrate–water–nitrate adduct within the dimeric cleft of the tripodal cations along with the relevant hydrogen bond interactions; (b) magnified view of the seven hydrogen bonding interactions of the nitrate anion (dashed lines) with four surrounding LH^+ units and the lattice water molecule (O13w).

$[\text{HL}^+][\text{ClO}_4^-]$ (**4**) crystallizes in the triclinic space group $P\bar{1}$ with $Z = 2$. The tripodal arms are orientated in a similar fashion to that of **2** with two arms in the folded conformation and the third arm orientated in the extended conformation (Table S4). Similar to **3**, there exist bifurcated ($\text{N}-\text{H}$) $^+ \cdots \text{O}$ interactions but the perchlorate oxygen atoms O11 and O13 involved in the electrostatic hydrogen bond formation come from two different perchlorate anions (N1...O11 2.860 Å, N1–H...O11 143°; N1...O13 2.990 Å, N1–H...O13 116°). In addition, there are seven C–H...O hydrogen bond contacts formed between the perchlorate oxygen atoms and different alkyl and aryl hydrogen atoms of the four coordinating tripodal units surrounding the anion with an average hydrogen bond length of 3.254 Å and a C–H...O angle range from 110–141°. An average C–H...O distance of

3.254 Å implies a better participation of the C–H donors towards perchlorate binding than nitrate. A magnified view of the perchlorate binding with the receptor is shown in Figure 5. The methylene protons H18B and H2B from the same cation interact with perchlorate oxygen atoms O10 and O11, respectively, whereas O12 of the perchlorate ion forms a bifurcated acceptor C–H...O hydrogen bond with the aliphatic hydrogen atom H17A and the aromatic hydrogen atom H15 of two different receptor units. Finally, O13 is involved in a trifurcated acceptor C–H...O hydrogen bond with the aliphatic protons H1B and H17B of the same tripodal cation and another H1B proton of a neighbouring cation. Thus, the nine-point attachment through strong (N–H)⁺...O and weak C–H...O interactions is responsible for the binding and stabilization of perchlorate with multiple protonated LH⁺ units. The details of the C–H...anion interactions are provided in Table S2. As observed in **2**, a bilayer arrangement of the ligand moiety is retained (Figure 4, b) by multiple interligand C–H...O_{nitro} interactions, an edge to face interaction (C–H...π) between the aryl hydrogen H5 with the phenyl ring involving carbon atoms C18–C24 (C3g) and a face to face interaction (π...π) between two identical phenyl rings (C3g) of successive tripodal units. Details of these interactions are provided in Table S3.

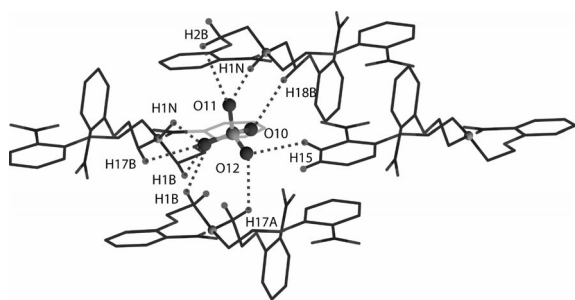


Figure 5. Magnified view of the nine hydrogen bond contacts between the perchlorate anion (dashed lines) and the four encircling LH⁺ units.

The silicon hexafluoride salt [HL⁺]₂[0.5SiF₆²⁻] (**5**) was obtained by reaction of the tripodal complex [L·HgCl₂] with (NH₄)₂SiF₆. The complex is a 2:1 ionic salt of L and H₂SiF₆, and crystallizes in the monoclinic space group *P*2₁/*n* with *Z* = 2. Interactions of the SiF₆²⁻ anion with the surrounding LH⁺ moieties comprise similar bifurcated (N–H)⁺...O intramolecular hydrogen bonding as observed in **3** (N1...F1 2.730 Å, N1–H...F1 152°; N1...F2 2.928 Å, N1–H...O13 129°). The fluoride atoms F2 and F3 each make three C–H...F hydrogen bond contacts, whereas F1 makes four contacts with the surrounding receptor moieties resulting in 24 hydrogen bonding contacts on SiF₆²⁻ together with four (N–H)⁺...O hydrogen bond interactions (Figure 6,a). An average hydrogen bond length of 3.271 Å implies the active participation of the alkyl and aryl C–H donors towards hexafluorosilicate binding through moderate C–H...F interactions. F1 is involved in aliphatic C–H...F interactions with the methylene hydrogen atoms H1B, H2A, H18A and H18B involving two different cations. Both F2

and F3 behave as trifurcated C–H...F hydrogen-bond acceptors, each interacting with two methylene and one aryl proton from the surrounding ligand moieties. The aliphatic protons H9B and H18B of one cation and the aryl hydrogen atom H24 from an adjacent LH⁺ unit make contacts with F2. Similarly, F3 is involved in an interaction with the aliphatic protons H1B and H2B and the aryl hydrogen atom H15 of two different tripodal cations. Details of the C–H...F interactions are provided in Table S2. The tripodal units in **5** pack into a bilayer structure (Figure 6, b) by effective intermolecular C–H...O_{nitro} interactions involving one or both of the oxygen atoms from each nitro group (O2, O6, O8 and O9) with the alkyl and aryl hydrogen atoms (H1A, H6, H14 and H21) and π...π interactions between the phenyl rings involving carbon atoms C3–C8 (C1g) and C11–C16 (C2g). In addition, the complex also demonstrates the formation of intermolecular C–H...O_{ether} hydrogen bonds between the aryl hydrogen atom H8 of one cation with the ethereal oxygen atom O7 of an adjacent tripodal cation. The details of these interactions are provided in Table S3.

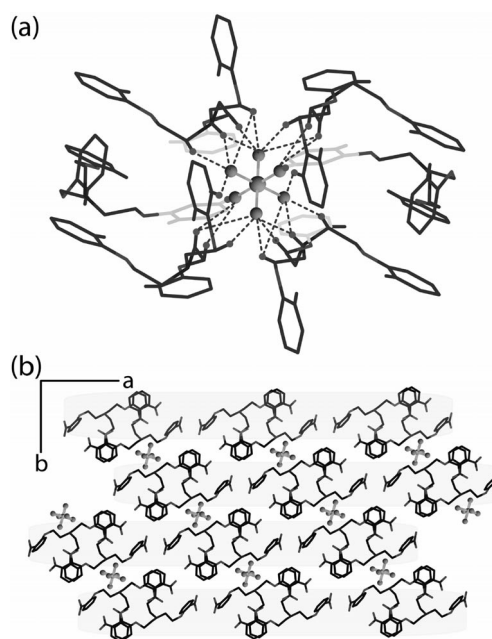


Figure 6. (a) Magnified view of the 24 hydrogen bonding interactions of hexafluorosilicate anion (dashed lines) with six encircling LH⁺ units; (b) crystal packing diagram of **5** viewed down the *c*-axis depicting the bilayer assembly formation of cationic ligand moieties along the *a*-axis with the SiF₆²⁻ anions sandwiched between the adjacent bilayers.

Rationalization of Structural Features

The hydrogen atom of the protonated bridgehead nitrogen in L is *exo*-orientated in all of the anion complexes and is involved in forming intramolecular (N–H)⁺...anion interactions with anions of different dimensionalities with hydrogen bond lengths ranging from 2.730 to 3.303 Å. The absence of intramolecular noncovalent interactions between

the receptor arms is likely to be responsible for the flat and extended orientation of the tripodal arms in the LH^+ units in the complexes.^[9] In all of these supramolecular complexes the anions are engaged in multiple weak $\text{C-H}\cdots\text{O}$ hydrogen bonds with methylene and aryl hydrogen atoms presented from the neighbouring tripodal cations. Protonation at the apical nitrogen and the presence of the electron withdrawing nitro functionality in the *ortho*-position of the terminal aryl render the methylene and aryl hydrogen atoms sufficiently acidic for their participation in weak $\text{C-H}\cdots\text{anion}$ interactions. Although not typically considered to be significant donors, there is increasing evidence that C-H groups can participate in hydrogen bonding and lead to enhanced anion binding affinity.^[10] This evidence comes in the form of direct observation of close contacts in crystallographic structures, anion induced chemical shifts of C-H protons in NMR spectra and theoretical calculations.^[11] The binding ability of tripodal receptors for anions varies with the functionality of the tripodal unit as functional groups modify the hydrogen bonding capability. A recent theoretical investigation by Hay et al. showed that the effect of electron withdrawing substituents on the aryl moiety significantly enhances the stability of anion complexes.^[12] Though charge neutralisation in the crystals and conventional hydrogen bonds are the main driving forces in the formation of supramolecular complexes, weak C-H hydrogen bonds provide added stabilization and satisfy the geometric needs of the LH^+ units by providing a favourable electrostatic environment around the anions. Moreover, interligand $\text{C-H}\cdots\text{O}_{\text{nitro}}$ interactions provide further stabilization to all anion complexes resulting in the bilayer assembly of ligand moieties in the solid state.

Studies on Anion Binding in Solution

To investigate the binding of different anions with the cationic receptor molecule in solution, we have protonated **L** with *p*-toluenesulfonic acid and monitored its spectral changes in the presence of various tetrabutylammonium (TBA) salts.^[13] The addition of an equivalent amount of TBA salts of Br^- , NO_3^- or ClO_4^- to a solution of $[\text{HL}^+][\text{Ts}]$ in CDCl_3 resulted in a notable upfield chemical shift of the aliphatic CH_2 proton resonances ($\Delta\delta = 0.048\text{--}0.053$ ppm), which indicates participation of the receptor in anion binding through weak hydrogen bonding interactions involving C-H protons (Supporting Information). Moreover, spectral changes were also observed for the aromatic C-H resonances. As most of the aliphatic $\text{CH}\cdots\text{anion}$ contacts are formed with the H atoms on carbon atoms adjacent to the ammonium ion, it can be argued that these H atoms are simply in the way due to the close approach of anions to the positively charged N atom and form electrostatic $(\text{N-H})^+\cdots\text{anion}$ interactions. The other possibility is that protonation at the apical nitrogen atoms renders the methylene CH_2 groups sufficiently acidic for their active participation towards anion binding by weak $\text{CH}\cdots\text{anion}$ interactions with an average C-H hydrogen bond length of 3.436 \AA . The

feeble nature of the C-H hydrogen bonds is reflected in the marginal upfield chemical shift of C-H proton resonances in ^1H NMR spectra and an average aliphatic/aromatic $\text{C-H}\cdots\text{anion}$ contact angle of 136° .

The binding properties of $[\text{HL}^+][\text{Ts}]$ with different anions in solution state were further investigated by ^1H NMR titration experiments in CDCl_3 at 298 K in the presence of $n\text{Bu}_4\text{N}^+\text{X}^-$ ($\text{X}^- = \text{Br}^-$, NO_3^- , ClO_4^-). Upon addition of aliquots from a stock solution of $n\text{Bu}_4\text{N}^+\text{X}^-$ (15 mM) to the initial solution of $[\text{HL}^+][\text{Ts}]$ (5 mM), a gradual upfield shift of the CH protons was observed (Supporting Information). The most substantial changes were observed for the aliphatic $-\text{CH}_2$ protons ($-\text{NCH}_2$ and $-\text{OCH}_2$), indicating that the aliphatic protons adjacent to the protonated nitrogen atom provide the maximum interaction between the receptor and anions. The upfield shift of the aliphatic protons with $\Delta\delta$ $-\text{NCH}_2$ ca. 0.052 and $-\text{OCH}_2$ ca. 0.056 ppm on addition of $n\text{Bu}_4\text{NBr}$, $\Delta\delta$ $-\text{NCH}_2$ ca. 0.044 and $-\text{OCH}_2$ ca. 0.049 ppm on addition of $n\text{Bu}_4\text{NNO}_3$ and $\Delta\delta$ $-\text{NCH}_2$ ca. 0.049 and $-\text{OCH}_2$ ca. 0.047 ppm on addition of $n\text{Bu}_4\text{NClO}_4$. The association constants (K) calculated for the anions by a nonlinear regression curve^[13e] indicate that bromide, nitrate and perchlorate bind only weakly with the protonated ligand having $\log K$ values of 0.245, 0.232 and 0.227 M^{-1} , respectively. Titration data gave the best fit for 1:1 association models of receptor to anion (Figure 7). The similar $\log K$ values suggest that, irrespective of their size and geometry (spherical Br^- , planar NO_3^- and tetrahedral ClO_4^-), the anions interact with the protonated receptor to almost the same extent. This is also evident from the structural studies of complexes **2**, **3** and **4** where the respective anions are involved in electrostatic $(\text{N-H})^+\cdots\text{anion}$ interactions with the concomitant formation of weak $\text{C-H}\cdots\text{anion}$ hydrogen bonds provided by four receptor units in each case.

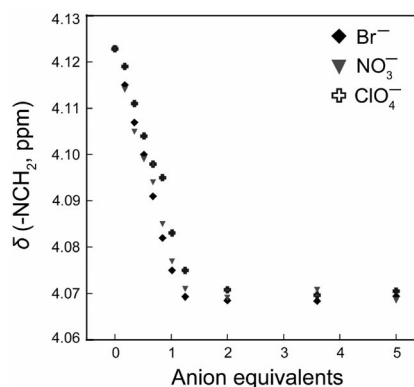


Figure 7. Plot of change in chemical shift of the aliphatic $-\text{NCH}_2$ protons of $[\text{HL}^+][\text{Ts}]$ with increasing addition of $n\text{Bu}_4\text{N}^+\text{X}^-$ ($\text{X}^- = \text{Br}^-$, NO_3^- , ClO_4^-) in CDCl_3 at 298 K.

Recovery of Receptor **L** from Anion Complexes

The receptor **L** can be recovered from the anion complexes in good yield simply by stirring a MeOH solution of the anion complex in the presence of excess Et_3N at room

temperature for about an hour. Evaporation of methanol under reduced pressure followed by extraction into CHCl₃ results in a yellow colouration of the organic layer due to the presence of **L**. Upon removal of CHCl₃, **L** is obtained as viscous oily liquid in greater than 85% yield. The receptor **L** can be dissolved in methanol and treated with HgCl₂ to afford the Hg^{II} complex again, this cycle is represented in Scheme 1.

Spectroscopic Evidence for the Formation of Anion Complexes

The transformation of [L·HgCl₂] into anion complexes followed by recovery of **L** has also been investigated in solution using UV/Vis and ¹H NMR spectroscopy. The electronic absorption spectrum of receptor **L** in methanol/H₂O

(9:1, v/v) shows a broad intraligand π - π^* transition band centred around 326 nm and an intense high energy absorption band centred at 259 nm (Figure 8, a). The absorption spectrum of [L·HgCl₂] shows a significant blueshift of 7 nm of the high energy absorption band but the peak position of the lower energy absorption band remains the same. Addition of NH₄Cl to the [L·HgCl₂] solution results in a considerable blueshift (ca. 5 nm) of the lower energy band with an isobestic point at 321 nm but the peak position of the high energy band (ca. 252 nm) remains the same with a gradual increase in its intensity (Figure 8, b). In order to validate the recovery of **L** in solution, we have monitored the absorption spectrum of **1** at a similar concentration. The peak positions of both absorption bands remain almost identical to that of the spectrum obtained upon titration of [L·HgCl₂] with NH₄Cl. Addition of Et₃N to a solution of **1** results in a redshift of 6 nm of the lower energy band with an isobestic point at 321 nm as observed in the previous process, and the peak position of the higher energy band (ca. 252 nm) remains the same with a gradual decrease in its intensity (Figure 8, c).

The excellent solubility of [L·HgCl₂] in MeCN allowed us to perform a ¹H NMR experiment in CD₃CN. A comparison of the ¹H NMR spectra of [L·HgCl₂] with that of **L** shows a downfield shift of the aliphatic CH₂ protons ($\Delta\delta = 0.07$ – 0.09 ppm) with marginal changes in the resonances of aromatic CH protons. The addition of 1 equiv. of NH₄Cl (D₂O solution) to the [L·HgCl₂] solution in CD₃CN results in a significant downfield shift of the aliphatic CH₂ resonances ($\Delta\delta = 0.48$ – 0.88 ppm), which indicates the influence of protonation at the apical nitrogen on the neighbouring methylene protons by extrusion of HgCl₂ (Figure 9). No-

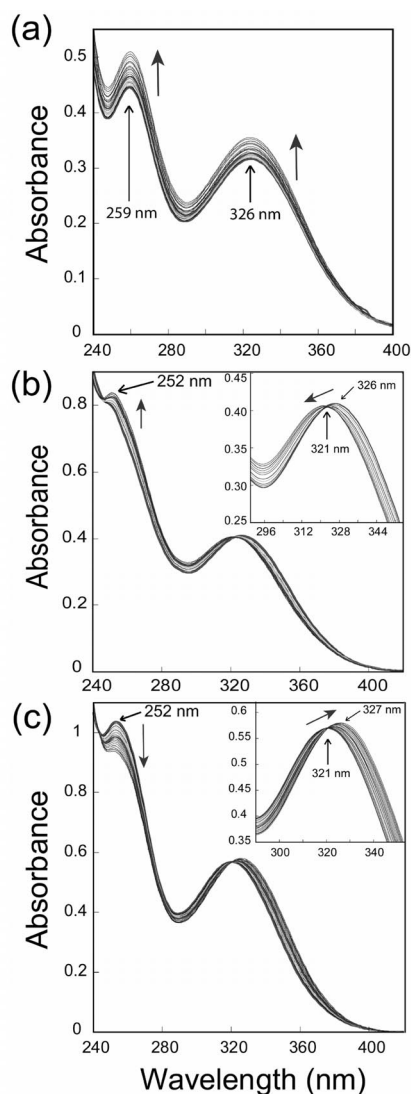


Figure 8. Absorption spectral changes of (a) **L** (10 μ M) upon addition of HgCl₂ solution in MeOH/H₂O (9:1, v/v); (b) [L·HgCl₂] (10 μ M) upon addition of NH₄Cl solution in MeOH/H₂O (9:1, v/v) and (c) **1** (10 μ M) upon addition of Et₃N solution in MeOH/H₂O (9:1, v/v).

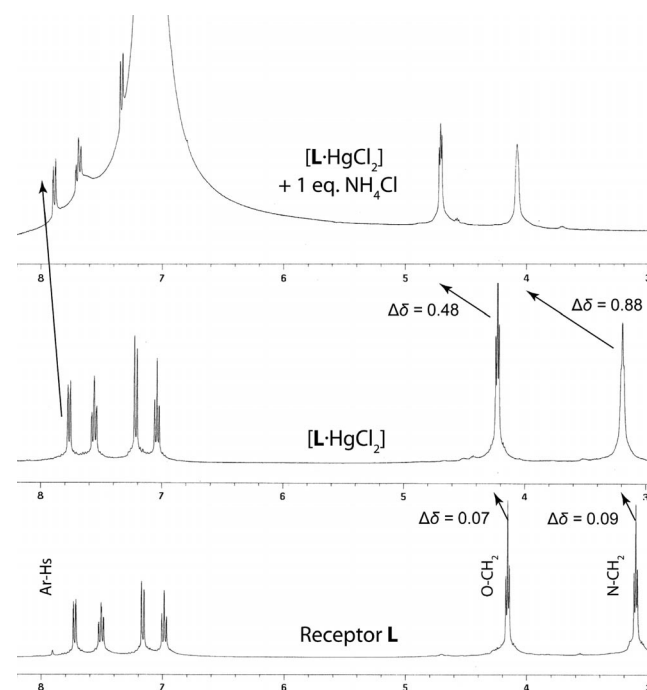


Figure 9. Partial ¹H NMR spectra (400 MHz, CD₃CN) of **L** (bottom), [L·HgCl₂] (middle) and [L·HgCl₂] with 1 equiv. of NH₄Cl in CD₃CN/D₂O (ca. 9:1) (top).

table downfield chemical shifts have also been observed for the aromatic CH protons. Thus, solution studies also give evidence for the formation of anion complexes from [L·HgCl₂] by extrusion of HgCl₂ employing ammonium salts as decomplexation agents.

Conclusions

In conclusion, we have been able to show the reversible complexation and decomplexation of HgCl₂ with a tripodal podand receptor bearing nitro functionality, employing readily available ammonium salts as Hg removal reagents. This study provides a new insight into the transformation of tripodal complexes of soft metal ions into supramolecular complexes including anions. We have also revealed solid state evidence for the active participation of both aliphatic CH₂ and aryl CH groups in the binding of different anions with **L**, exhibiting aliphatic C–H···anion hydrogen bond strengths comparable to those of aryl C–H···anion hydrogen bonds. These hydrogen bonds are also actively involved in providing further stabilization to the complexes by forming directional interligand C–H···O_{nitro} hydrogen bonds with the oxygen atoms of the nitro groups establishing a bilayer structure in the solid state. A detailed structural investigation clearly demonstrates that the self-alignment, flexibility and orientation of the ligand moiety play a crucial role in making a variety of molecular interactions possible in the binding of HgCl₂ and anions of different dimensionality. Therefore, complexes with **L** provide excellent examples of Hg^{II} complexation and C–H···anion hydrogen bonding in anion complexes.

Experimental Section

Materials and Methods: All reagents and solvents were obtained from commercial sources and used as received unless specified. NMR spectra were recorded with a Varian FT-400 MHz instrument. Chemical shifts were recorded in ppm using tetramethylsilane (TMS) as a reference. IR spectra were recorded with a Perkin–Elmer–Spectrum One FT-IR spectrometer as KBr disks in the range 4000–450 cm⁻¹. Absorption spectra were recorded with a Perkin–Elmer Lambda-25 UV/Vis spectrometer at 298 K. Elemental analyses were carried out with a Perkin–Elmer 2400 automatic carbon, hydrogen and nitrogen analyzer.

Synthesis of Tripodal Receptor L: The receptor **L** was synthesized by modification of our recent literature procedure.^[14] To a solution of 2-nitrophenol (5 g, 36 mmol) in dry *n*-propanol (30 mL) was added crushed NaOH (1.77 g, 43 mmol), and the solution was stirred at room temperature for 1 h. To the resulting suspension was added tris(2-chloroethyl)amine hydrochloride (2.88 g, 12 mmol) at once, and the mixture was stirred for another 1 h at room temperature and then heated to reflux for 8 h. The solvents were removed under reduced pressure and cold water (20 mL) was added. The product was extracted into CHCl₃ (3 × 20 mL) and the organic layer was washed with water and dried with anhydrous Na₂SO₄ before the solvents were removed under reduced pressure. The crude product was purified by column chromatography with 75% ethyl acetate (in petroleum ether) as the eluent. The product was a viscous brown liquid. Yield: 66% (1.40 g). ¹H NMR (400 MHz,

CD₃CN): δ = 3.10 (t, *J* = 5.4 Hz, 6 H, NCH₂), 4.15 (t, *J* = 5.4 Hz, 6 H, OCH₂), 6.98 (t, *J* = 7.8 Hz, 3 H, ArH), 7.16 (d, *J* = 8.8 Hz, 3 H, ArH), 7.50 (t, *J* = 5.6 Hz, 3 H, ArH), 7.71 (d, *J* = 8.0 Hz, 3 H, ArH) ppm. ¹³C NMR (100 MHz, CD₃CN): δ = 54.85 (×3 C, NCH₂), 69.94 (×3 C, OCH₂), 115.89 (×3 C, ArH), 121.28 (×3 C, ArH), 126.10 (×3 C, ArH), 135.29 (×3 C, ArH), 140.79 (×3 C, ArH), 152.91 (×3 C, ArH) ppm.

Synthesis of [L·HgCl₂]: The Hg complex was synthesized by adding a solution of HgCl₂ (0.458 g, 1.95 mmol) in methanol (10 mL) to a well stirred solution of **L** (1 g, 1.95 mmol) in methanol (20 mL) at room temperature. The mixture was stirred for 3 h during which a light yellow precipitate was formed. The volume of the solution was reduced to ca. 10 mL. The precipitate was collected by filtration under cold conditions and washed with diethyl ether and dried in a vacuum desiccator. Yield: 72% (1.10 g) based on **L**. Single crystals suitable for X-ray analysis were grown from an acetonitrile solution over 1 week. ¹H NMR (400 MHz, CD₃CN): δ 3.19 (t, *J* = 4.8 Hz, 6 H, NCH₂), 4.22 (t, *J* = 5.2 Hz, 6 H, OCH₂), 7.04 (t, *J* = 7.6 Hz, 3 H, ArH), 7.21 (d, *J* = 8.8 Hz, 3 H, ArH), 7.54 (t, *J* = 7.2 Hz, 3 H, ArH), 7.77 (d, *J* = 8.0 Hz, 3 H, ArH) ppm. ¹³C NMR (100 MHz, CD₃CN): δ = 55.68 (×3 C, NCH₂), 65.62 (×3 C, OCH₂), 116.34 (×3 C, ArH), 122.77 (×3 C, ArH), 126.89 (×3 C, ArH), 136.22 (×3 C, ArH), 140.59 (×3 C, ArH), 152.03 (×3 C, ArH) ppm. C₂₄H₂₄Cl₂HgN₄O₉ (783.96): calcd. C 36.76, H 3.08, N 7.14; found C 35.24, H 2.59, N 7.35.

Synthesis Complexes 1–5: Anion complexes **1–5** were synthesized by reacting [L·HgCl₂] with equivalent amounts of NH₄Cl, NH₄Br, NH₄NO₃, NH₄ClO₄ or (NH₄)₂SiF₆. As (NH₄)₂SiF₆ cannot be obtained commercially, this was prepared by reacting an aqueous 30% ammonia solution with HF in a glass beaker. To form the complexes, [L·HgCl₂] (100 mg) was dissolved in MeOH (20 mL) and 1 equiv. of the ammonium salt dissolved in minimum volume of water (ca. 2 mL) was added at once. The solution mixture was then stirred with gentle heating (ca. 60 °C) for about 4 h, allowed to cool to room temp. and filtered. Slow evaporation of the filtrate at room temp. yielded colourless block/rectangular crystals suitable for X-ray analysis.

[HL⁺][Cl⁻] (1): Colourless crystals; yield of crystallization: 82% (58 mg) based on [L·HgCl₂]; mp: 175 °C; ¹H NMR (400 MHz, [D₆]DMSO): δ = 3.90 (s, 6 H, NCH₂), 4.68 (s, 6 H, OCH₂), 7.17 (t, *J* = 7.2 Hz, 3 H, ArH), 7.39 (d, *J* = 8.4 Hz, 3 H, ArH), 7.70 (t, *J* = 6.8 Hz, 3 H, ArH), 7.92 (d, *J* = 8.0 Hz, 3 H, ArH) ppm. IR (KBr disk): ν̄ = 1242, 1519, 1606, 3422 cm⁻¹. C₂₄H₂₅ClN₄O₉ (548.93): calcd. C 52.51, H 4.59, N 10.20; found C 52.98, H 4.13, N 9.56.

[HL⁺][Br⁻] (2): Colourless crystals; yield of crystallization: 76% (56 mg) based on [L·HgCl₂]; mp: 198 °C; ¹H NMR (400 MHz, [D₆]DMSO): δ = 3.54 (s, 6 H, NCH₂), 4.65 (s, 6 H, OCH₂), 7.15 (t, *J* = 7.8 Hz, 3 H, ArH), 7.37 (d, *J* = 8.4 Hz, 3 H, ArH), 7.68 (t, *J* = 7.8 Hz, 3 H, ArH), 7.89 (d, *J* = 8.0 Hz, 3 H, ArH) ppm. IR (KBr disk): ν̄ = 1272, 1526, 1609, 3444 cm⁻¹. C₂₄H₂₅BrN₄O₉ (593.38): calcd. C 48.57, H 4.24, N 9.44; found C 48.49, H 4.58, N 9.25.

[HL⁺][NO₃⁻]·0.5H₂O (3): Colourless crystals; yield of crystallization: 80% (115 mg) based on [L·HgCl₂]; mp: 192 °C; ¹H NMR (400 MHz, [D₆]DMSO): δ = 3.89 (s, 6 H, NCH₂), 4.57 (s, 6 H, OCH₂), 7.15 (t, *J* = 6.8 Hz, 3 H, ArH), 7.36 (d, *J* = 8.0 Hz, 3 H, ArH), 7.68 (t, *J* = 7.2 Hz, 3 H, ArH), 7.89 (d, *J* = 7.2 Hz, 3 H, ArH) ppm. IR (KBr disk): ν̄ = 1278, 1384, 1526, 1607, 3436 cm⁻¹. C₂₄H₂₆N₅O_{12.5} (583.49): calcd. C 50.00, H 4.55, N 12.15; found C 49.88, H 4.26, N 11.76.

[HL⁺][ClO₄⁻] (4): Colourless crystals; yield of crystallization: 75% (58 mg) based on [L·HgCl₂]; mp: 181 °C; ¹H NMR (400 MHz, [D₆]DMSO): δ = 3.89 (s, 6 H, NCH₂), 4.55 (s, 6 H, OCH₂), 7.15 (t, *J* = 7.8 Hz, 3 H, ArH), 7.32 (d, *J* = 8.4 Hz, 3 H, ArH), 7.66 (t, *J* = 7.6 Hz, 3 H, ArH), 7.86 (d, *J* = 8.0 Hz, 3 H, ArH) ppm. IR (KBr disk): $\tilde{\nu}$ = 1085, 1274, 1526, 1609, 3110 cm⁻¹. C₂₄H₂₅ClN₄O₁₃ (612.93); calcd. C 47.02, H 4.11, N 9.14; found C 46.84, H 4.42, N 9.26.

[HL⁺][0.5SiF₆⁻²] (5): Colourless crystals; yield of crystallization: 76% (110 mg) based on [L·HgCl₂]; mp: 207 °C; ¹H NMR (400 MHz, [D₆]DMSO): δ = 4.39 (s, 6 H, OCH₂), 7.12 (t, *J* = 7.6 Hz, 3 H, ArH), 7.34 (d, *J* = 8.4 Hz, 3 H, ArH), 7.65 (t, *J* = 7.2 Hz, 3 H, ArH), 7.86 (d, *J* = 8.0 Hz, 3 H, ArH) ppm. IR (KBr disk): $\tilde{\nu}$ = 1274, 1528, 1607, 3436 cm⁻¹. C₂₄H₂₅F₃N₄O₉Si_{0.5} (584.52); calcd. C 50.53, H 4.42, N 9.82; found C 50.84, H 4.22, N 9.48.

Single-Crystal X-ray Studies: The crystallographic data and details of data collection and refinement for [L·HgCl₂] and **1–5** are given in Table S1 in the Supporting Information. In each case, a single crystal of suitable size was selected from the mother liquor at room temp. immersed in Paratone oil and then mounted on the tip of a glass fibre and cemented using epoxy resin. The intensity data were collected using a Bruker SMART APEX-II CCD diffractometer, equipped with a fine focus 1.75 kW sealed tube Mo-*K*_α radiation (λ = 0.71073 Å) at 298(3) K, with increasing ω (width of 0.3° per frame) at a scan speed of 6 s/frame. SMART software was used for data acquisition. Data integration and reduction were undertaken with SAINT and XPREP^[15] software. Multiscan empirical absorption corrections were applied to the data using the program SADABS.^[16] Structures were solved by direct methods using SHELXS-97^[17] and refined with full-matrix least-squares on *F*² using SHELXL-97.^[18] All non-hydrogen atoms were refined anisotropically. Hydrogen atoms attached to all carbon atoms were geometrically fixed whereas the hydrogen atoms of the tertiary amino nitrogen of the salts were located from the difference Fourier map, and the positional and temperature factors are refined isotropically. However, we were unable to locate the hydrogen atoms of the lattice water molecule in **3** from the difference Fourier map. Structural illustrations have been generated using ORTEP-3^[19] and MERCURY 1.3^[20] for Windows.

¹H NMR Titration Experiments: Binding constants were obtained by ¹H NMR (400 MHz, Bruker) titrations of [HL⁺][Ts] with tetrabutylammonium salts in CDCl₃ at 25 °C. The initial concentration of receptor was 5 mM. Aliquots of anions were added from a stock solution 15 mM of anions. TMS in CDCl₃ was used as an internal reference, and each titration was performed by 10 measurements at room temperature. All the proton signals were referred to TMS. Association constants were calculated by fitting the change in the N-CH₂ chemical shift with a 1:1 association model with nonlinear least square analysis. WINEQNMR 2.0 was employed in the calculation of association constants.^[21] The error limit in *K* was about 10%.

The following equation was used to determine *K* values, where *A* and *R* are the anion and [HL⁺][Ts], respectively.

$$\Delta\delta = \{([A]_0 + [R]_0 + 1/K) \pm \sqrt{([A]_0 + [R]_0 + 1/R)^2 - 4[R]_0[A]_0}\}^{1/2} - \Delta\delta_{\max}/2[R]_0$$

Supporting Information (see also the footnote on the first page of this article): Further crystallographic details involving tables of the crystal structure determination, selected hydrogen bond parameters and selected torsion angles, ¹H NMR spectra and titrations, thermal ellipsoid plots (50% probability model) of complexes **1–5** and packing diagrams.

Acknowledgments

G. D. acknowledges the Department of Science and Technology (DST), Grant No. SR/S1/IC-01/2008 and the Council of Scientific and Industrial Research (CSIR), Grant No. 01-2235/08/EMR-II, New Delhi, India for financial support and DST-FIST for single-crystal X-ray diffraction measurements. S. K. D. acknowledges IIT Guwahati, India for a fellowship.

- a) D. J. Cram, *Science* **1983**, *219*, 1177–1182; b) R. Warmuth, J. Yoon, *Acc. Chem. Res.* **2001**, *34*, 95–105; c) J. Rebek Jr., *Acc. Chem. Res.* **1999**, *32*, 278–286; d) A. Shivanyuk, J. Rebek Jr., *J. Am. Chem. Soc.* **2002**, *124*, 12074–12075; e) T. Amaya, J. Rebek Jr., *Chem. Commun.* **2004**, 1802–1803; f) A. S. Singh, P. K. Bharadwaj, *Dalton Trans.* **2008**, 738–741; g) S. Rieth, Z. Yan, S. Xia, M. Gardlik, A. Chow, G. Fraenkel, C. M. Hadad, J. D. Badjic, *J. Org. Chem.* **2008**, *73*, 5100–5109; h) A. Kumar, S.-S. Sun, A. J. Lees, *Coord. Chem. Rev.* **2008**, *252*, 922–939.
- a) A. Bianchi, K. Bowman-James, E. Garcia-Espana, *Supramolecular Chemistry of Anions*; Wiley-VCH, Weinheim, Germany, **1997**; b) S. S. Zhu, H. Staats, K. Brandhorst, J. Grunenberg, F. Gruppi, E. Dalcana, A. Lutzen, K. Rissanen, C. A. Schalley, *Angew. Chem. Int. Ed.* **2008**, *47*, 788–792; c) M. J. Chmielewski, L. Zhao, A. Brown, D. Curiel, M. R. Sambrook, A. L. Thompson, S. M. Santos, V. Felix, J. J. Davis, P. D. Beer, *Chem. Commun.* **2008**, 3154–3156; d) M. D. Lankshear, P. D. Beer, *Acc. Chem. Res.* **2007**, *40*, 657–665; e) N. Gimeno, R. Vilar, *Coord. Chem. Rev.* **2006**, *250*, 3161–3189; f) S. J. Coles, J. G. Frey, P. A. Gale, M. B. Hursthouse, M. E. Light, K. Navakhun, G. L. Thomas, *Chem. Commun.* **2003**, 568–569; g) J. L. Atwood, A. Szumna, *Chem. Commun.* **2003**, 940–941; h) R. L. Paul, Z. R. Bell, J. C. Jeffery, J. A. McCleverty, M. D. Ward, *Proc. Natl. Acad. Sci. USA* **2002**, *99*, 4883–4888; i) D. Rais, J. Yau, D. M. P. Mingos, R. Vilar, A. J. P. White, D. J. Williams, *Angew. Chem. Int. Ed.* **2001**, *40*, 3464–3467; j) R. Vilar, D. M. P. Mingos, A. J. P. White, D. J. Williams, *Angew. Chem. Int. Ed.* **1998**, *37*, 1258–1262.
- a) D. H. Busch, N. A. Stephenson, *Coord. Chem. Rev.* **1990**, *100*, 119–154; b) S. Anderson, H. L. Anderson, J. K. M. Sanders, *Acc. Chem. Res.* **1993**, *26*, 469–475; c) R. Vilar, *Angew. Chem. Int. Ed.* **2003**, *42*, 1460–1477.
- a) A. S. Singh, P. K. Bharadwaj, *Dalton Trans.* **2008**, 738–741; b) A. S. Singh, B. Chen, Y. Wen, C. Tsai, S. Sun, *Org. Lett.* **2009**, *11*, 1867–1870.
- a) M.-R. Huang, X.-G. Li, *Chem. Eur. J.* **2007**, *13*, 6009–6018, and references cited therein; b) L. Praveen, G. R. Thirumalai, T. Sreeja, M. L. P. Reddy, R. L. Varma, *Inorg. Chem.* **2007**, *46*, 6277–6282; c) G. K. Patra, I. Goldberg, *Polyhedron* **2002**, *21*, 2195–2199; d) D. C. Bebout, S. W. Stokes, R. J. Butcher, *Inorg. Chem.* **1999**, *38*, 1126–1133; e) D. A. House, W. T. Robinson, V. McKee, *Coord. Chem. Rev.* **1994**, *135/136*, 533–585; f) G. A. Bowmaker, B. Assadollahzadeh, A. M. Brodie, E. W. Ainscough, G. H. Freeman, G. R. Jameson, *Dalton Trans.* **2005**, 1602–1612; g) D. G. Morris, K. W. Muir, C. O. W. Chii, *Polyhedron* **2003**, *22*, 3345–3353.
- a) A. Oehmen, R. Viegas, S. Velizarov, M. A. M. Reis, J. G. Crespo, *Desalination* **2006**, *199*, 405; b) A. Kowalski, *Metals Removal to Low Levels Using Precipitants*, presented at the AESF/EPA Conference, Orlando, FL, January 28–30, **2002**.
- M. Arunachalam, P. Ghosh, *Chem. Commun.* **2009**, 3184–3186.
- a) A. Pramanik, S. Majumdar, G. Das, *CrystEngComm* **2010**, *12*, 250; b) S. K. Dey, B. Ojha, G. Das, *Cryst. Eng. Commun.* **2010**; DOI: 10.1039/c0ce00316f.
- a) P. S. Lakshminarayanan, I. Ravikumar, E. Suresh, P. Ghosh, *Inorg. Chem.* **2007**, *46*, 4769–4771; b) A. Pramanik, M. Bhuyan, R. Choudhury, G. Das, *J. Mol. Struct.* **2008**, *879*, 88–95; c) M. A. Hossain, J. A. Liljegen, D. Powell, K. A. Bowman-James, *Inorg. Chem.* **2004**, *43*, 3751–3755.

- [10] a) R. K. Castellano, *Curr. Org. Chem.* **2004**, *8*, 845–865; b) Z. Xu, S. K. Kim, J. Yoon, *Chem. Soc. Rev.* **2010**, *39*, 1457–1466.
- [11] a) K. J. Wallace, W. J. Belcher, D. R. Turner, K. F. Syed, J. W. Steed, *J. Am. Chem. Soc.* **2003**, *125*, 9699–9715; b) C. A. Ilioudis, D. A. Tocher, J. W. Steed, *J. Am. Chem. Soc.* **2004**, *126*, 12395–12402; c) D. R. Turner, E. C. Spencer, J. A. K. Howard, D. A. Tocher, J. W. Steed, *Chem. Commun.* **2004**, 1352–1353; d) M. J. Chmielewski, M. Charon, J. Jurczak, *Org. Lett.* **2004**, *6*, 3501–3504; e) S. O. Kang, D. VanderVelde, D. Powell, K. Bowman-James, *J. Am. Chem. Soc.* **2004**, *126*, 12272–12273; f) J. Y. Kwon, Y. J. Jang, S. K. Kim, K.-H. Lee, J. S. Kim, J. Yoon, *J. Org. Chem.* **2004**, *69*, 5155–5157; g) A. M. Costero, M. J. Banuls, M. J. Aurell, M. D. Ward, S. Argent, *Tetrahedron* **2004**, *60*, 9471–9478; h) S. Ghosh, A. R. Choudhury, T. N. G. Row, U. Maitra, *Org. Lett.* **2005**, *7*, 1441–1444; i) K. Hiraoka, S. Mizuse, S. Yamabe, *Chem. Phys. Lett.* **1988**, *147*, 174; j) Z. M. Loh, R. L. Wilson, D. A. Wild, E. J. Bieske, *J. Chem. Phys.* **2003**, *119*, 9559–9567; k) F. M. Raymo, M. D. Bartberger, K. N. Houk, J. F. Stoddart, *J. Am. Chem. Soc.* **2001**, *123*, 9264–9267.
- [12] a) V. S. Bryantsev, B. P. Hay, *Org. Lett.* **2005**, *7*, 5031–5034; b) O. B. Berryman, V. S. Bryantsev, D. P. Stay, D. W. Johnson, B. P. Hay, *J. Am. Chem. Soc.* **2007**, *129*, 48–58; c) B. P. Hay, V. S. Bryantsev, *Chem. Commun.* **2008**, 2417–2428.
- [13] a) M. A. Saeed, J. J. Thompson, F. R. Fronczekb, M. A. Hossain, *CrystEngComm* **2010**, *12*, 674–676; b) M. A. Saeed, F. R. Fronczekb, M. A. Hossain, *Chem. Commun.* **2009**, 6409–6411; c) M. A. Saeed, F. R. Fronczekb, M. Huang, M. A. Hossain, *Chem. Commun.* **2010**, 404–406; d) J. S. Mendy, M. L. Pilate, T. Horne, V. W. Dayb, M. A. Hossain, *Chem. Commun.* **2010**, 6084–6086; e) P. Morehouse, M. A. Hossain, J. M. Llinares, D. Powell, K. Bowman-James, *Inorg. Chem.* **2003**, *42*, 8131–8133.
- [14] S. K. Dey, G. Das, *Cryst. Growth Des.* **2010**, *10*, 754–760.
- [15] SAINT, SMART and XPREP, *Siemens Analytical X-ray Instruments Inc.*, Madison, Wisconsin, USA, **1995**.
- [16] G. M. Sheldrick, *SADABS: Software for Empirical Absorption Correction*, University of Göttingen, Göttingen, Germany, **1999–2003**.
- [17] G. M. Sheldrick, *SHELXS-97*, University of Göttingen, Germany, **1997**.
- [18] G. M. Sheldrick, *SHELXL-97, Program for Crystal Structure Refinement*, University of Göttingen, Germany, **1997**.
- [19] L. J. Farrugia, *J. Appl. Crystallogr.* **1997**, *30*, 565–566.
- [20] *Mercury 1.3 Supplied with Cambridge Structural Database*, CCDC, Cambridge, U. K., **2003–2004**.
- [21] M. J. Hynes, *J. Chem. Soc., Dalton Trans.* **1993**, 311–312.

Received: July 30, 2010

Published Online: December 10, 2010